Characterization of electrowetting actuation on addressable single-side coplanar electrodes

2006 J. Micromech. Microeng. 16 2053

(http://iopscience.iop.org/0960-1317/16/10/018)

INSTITUTE OF PHYSICS PUBLISHING JOURNAL OF MICROMECHANICS AND MICROENGINEERING

J. Micromech. Microeng. **16** (2006) 2053–2059 doi:10.1088/0960-1317/16/10/018

Characterization of electrowetting actuation on addressable single-side coplanar electrodes

Ui-Chong Yi[1] **and Chang-Jin Kim**

Mechanical and Aerospace Engineering Department, University of California, Los Angeles (UCLA), CA, USA

E-mail: uyi@coremicrosolutions.com

Received 27 April 2006, in final form 22 June 2006
Published 25 August 2006
Online at stacks.iop.org/JMM/16/2053

Abstract

This paper studies and characterizes electrowetting-on-dielectric (EWOD) actuations on coplanar electrodes with an electrode-free cover plate or no cover plate. By arranging driving and reference electrodes on one plate, such an EWOD configuration can accommodate more sensing mechanisms from above and thus allows increased flexibility for system development. Various coplanar electrodes are tested for contact angle changes by EWOD with a focus on the effect of the percentage gap between electrodes and are found to be in good agreement with a simple analytical model. The droplet-moving devices demonstrate the successful moving, cutting and merging of droplets (∼0.1 μl) in a parallel-plate configuration, i.e., between the driving plate with coplanar electrodes and the passive plate with no electrode. EWOD actuation in single plate configuration, i.e. no cover plate, is also demonstrated, adding additional flexibility for the system design.

(Some figures in this article are in colour only in the electronic version)

1. Introduction

Microfluidic technology plays a critical role in lab-on-a-chip systems, or micro-total analysis systems (μ-TAS) [1, 2], by delivering chemical or biological samples and reagents to processing components for data collections or on-chip sample preparations. Currently, the majority of lab-on-a-chip systems rely on a continuous microfluidics flowing liquid through fixed passages (e.g., microchannels) by an electrokinetic driving or by a pressure source on or off chip. A new approach in microfluidics, at times called 'digital microfluidics', uses discrete volumes of fluids rather than channel-based continuous flows. Although first demonstrated by discrete vapor bubbles in a liquid-filled microchannel [3], the complementary state of liquid droplets in a gas environment is far more common today for digital microfluidics, as the demands for microfluidics have been dominated by biomedical and chemical applications. The droplet can be moved by various actuation methods, including thermal [4], surface wave [5], electrostatic [6], dielectrophoretic [7] and, most commonly, electrowetting [8, 9]. A common feature of the droplet-driving schemes is that the actuations are local. Since no pressure is needed, digital microfluidic systems can be built without microchannels, pressure sources (e.g., micropumps) or regulatory elements (e.g., microvalves). This greatly simplifies the device and system both in design and fabrication. The simplicity further presents additional unique opportunities such as the reduction of dead volumes and the possibility of portable systems.

For electrowetting actuation, the configuration of electrowetting-on-dielectric (EWOD), as opposed to the historically known electrowetting on a metal, has become the choice for aqueous liquids for its reversible operations [8]. Demonstrated to manipulate aqueous droplets in air [8, 10] and oil [9], EWOD-based microfluidics development has reported many physical functions: creating, dividing and merging droplets [10]; mixing different droplets [11, 12]; separating and concentrating particles in a droplet [13]; and droplet printing [14]—all with little additional complications to the device. With the ability to create EWOD chips capable

[1] Currently with Core Microsolutions, Inc. LA, CA USA.

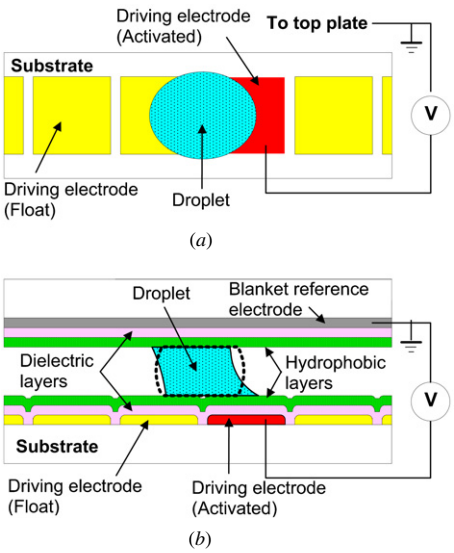

Figure 1. Popular two-plate configuration EWOD chip with asymmetric electrode arrangement. Once voltage is applied, the change in the meniscus shape (from the dotted shape) caused by contact angle changes induces a gradient inside the droplet. (*a*) Top view; (*b*) cross-section view.

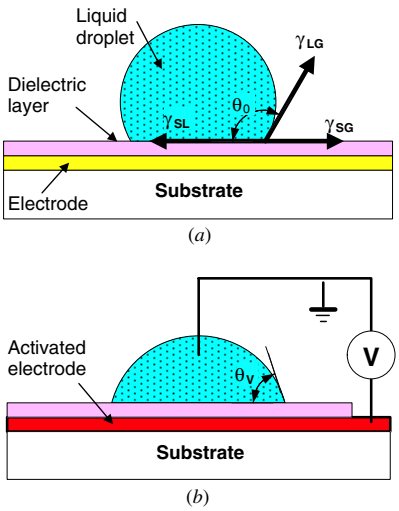

Figure 2. Contact angle changes by electrical potential on the EWOD surface: (*a*) initial state; (*b*) activated state.

of manipulating multiple droplets on a two-dimensional grid array [15] and to build an entire system on a printed circuit board [16], a complete hand-held lab-on-a-chip system seems within the horizon.

A popular configuration of EWOD chip today uses two parallel plates: a top plate with a fixed blanket referencing electrode and a bottom plate with patterned addressable driving electrodes (figure 1). Both electrodes are covered with an insulating layer (e.g., SiO_2 and Parylene®), which is, in turn, coated with a hydrophobic layer (e.g., Teflon® and Cytop®). A liquid droplet is squeezed in between the two plates, forming the initial droplet shape drawn in dotted lines in figure 1. Once electrical potential is applied between the top reference electrode and the bottom driving electrode at the droplet edge, the contact angles change accordingly, generating a pressure gradient inside the droplet and driving it [8, 9]. The top reference electrode is essential for stable actuation since it provides the ground for the potential drops across insulating layers.

Although the two-plate configuration provides many advantages (e.g., reliable droplet volume control, gravity insensitivity), one drawback is the difficulty in integrating additional functions on the chip (e.g., sensing devices) without impacting electrode area/arrangement or interfering with EWOD actuation. While optical sensing or actuation is compatible because it can be added off chip by using transparent plates (e.g., glass coated with indium tin oxide (ITO) electrodes), other mechanisms face steeper challenges in integration onto the EWOD chip. It would be most desirable if the top plate has no role in EWOD actuation, so that other functions can be built on or operate through the plate. To obtain the above goal, in this paper, we develop and characterize a EWOD plate containing both the driving and reference electrodes coplanar. Although coplanar placement of both electrodes on one plate has been known, as mentioned for a two-plate configuration [9] or demonstrated for one-plate (i.e., no cover plate) [17], the idea has not been studied or tested in any detail.

By putting all the electrodes necessary for EWOD actuation on one plate, the other plate can independently accommodate other various mechanisms, such as electrochemical, mechanical and optical sensing. Or the EWOD device can be designed without a cover plate for some applications. Furthermore, we expect the coplanar electrode design will help building stacked EWOD chips, which we envision for future EWOD devices with increased capacities. With these future directions in mind, we verify the coplanar electrodes, analyze the EWOD mechanism on them, characterize the performance for various electrode designs and demonstrate common droplet operations, expanding from our preliminary result [18].

2. EWOD actuation without the top reference electrode

2.1. Contact angle change on coplanar electrodes

Electrowetting enables the control of surface wettability by changing the surface free energy through applied potentials. Figure 2 illustrates the case of a sessile drop for EWOD, where electric potential is applied between the liquid and the electrodes embedded underneath a dielectric layer. When a voltage is applied, the contact angle of the liquid is decreased (figure 2(*b*)) from its initial contact angle (figure 2(*a*)). The relation between applied voltages and contact angle changes can be formulated by combining Lippmann's equation and Young's equation:

$$\cos\theta_V - \cos\theta_0 = \frac{\varepsilon_r \varepsilon_0}{2\gamma_{LG} t} V^2 \qquad (1)$$

where θ_V and θ_0 are corresponding contact angles at applied voltage V and 0 V, respectively, ε_r and ε_0 are the dielectric constant of the insulating layer and the permittivity of vacuum, respectively, γ_{LG} is liquid–gas interfacial energy and t is the thickness of the dielectric layer [19].

If a voltage is applied between two electrodes placed *coplanar* on the surface (figure 3(*b*)), equation (1) needs to

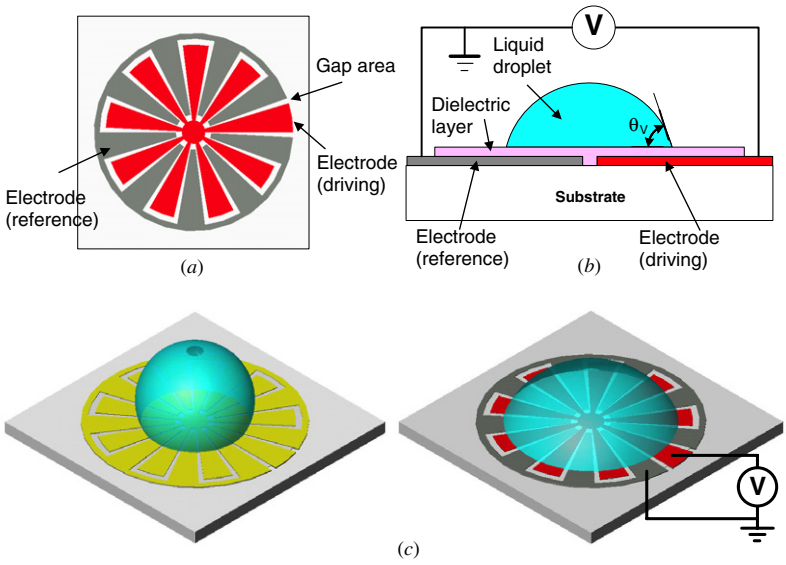

Figure 3. EWOD of a sessile drop on single-side coplanar electrodes: (*a*) electrode arrangement (top view); (*b*) cross-section view with voltage applied; (*c*) contact angle change on coplanar electrodes.

be modified to account for the gap areas of insulating material between the adjacent electrodes (figure 3(*a*)). By assuming that the area of each sub-electrode (e.g. ground or signal electrode) covered by the droplet is much smaller than the total area covered by the droplet and thus averaging the changes in interfacial energy above the electrodes and the gap area, the dependence of the solid–liquid interfacial tension γ_{SL} at applied voltage V is modified from the original Lippmann's equation as

$$\gamma_{SL}(V) - \gamma_{SL}(0) = -\frac{\varepsilon_r \varepsilon_0}{2t}\left(\frac{A_d}{A_t}V_d^2 + \frac{A_r}{A_t}V_r^2 + \frac{A_g}{A_t}V_g^2\right) \quad (2)$$

where $\gamma_{SL}(0)$ is the interfacial tension with no voltage applied, A_d, A_r and A_g are the areas over the driving electrodes, the reference electrodes and the gap areas between the electrodes, respectively, A_t is the total combined area, and V_d, V_r and V_g are voltages across the dielectric layer above each respective area. The values of V_d and V_r are inversely proportional to their relative ratio of the area. In equation (2), $V_g = 0$ V because no electrode is embedded underneath the gap area. Combining equation (2) with Young's equation, we obtain the relation between the applied voltage and the contact angle change for the coplanar electrode design[2]:

$$\cos\theta_V - \cos\theta_0 = \frac{\varepsilon_r \varepsilon_0}{2\gamma_{LG}t}\left(\frac{A_d}{A_t}\left(\frac{A_r}{A_d + A_r}\right)^2 + \frac{A_r}{A_t}\left(\frac{A_d}{A_d + A_r}\right)^2\right)V^2 \quad (3)$$

As seen in equation (3), the contact angle changes are related to the area ratio among driving electrodes, reference electrodes and the gaps between them. To maximize the angle changes, the modifying geometric factor in the large bracket in the equation needs to be optimized; for a given voltage, the maximum angle changes are obtained when A_d and A_r are equal and A_g is minimized. This maximum value is 25% of the figure 2 case and about 50% of what the two-plate configuration of figure 1 would allow.

[2] A similar expression was reported by Kwon and Lee [20].

2.2. *Driving a droplet on coplanar electrodes in a parallel-plate configuration with a passive top plate*

Similar to the modification made to equation (1) to reach equation (3) for the sessile drop cases of figures 2 and 3, the equation describing the EWOD driving pressure on the coplanar electrodes under the parallel-plate configuration of figure 1 needs to be modified accordingly. In the coplanar electrode configuration, one driving unit is composed of multiple coplanar sub-electrodes, as shown in figure 4(*a*). By applying potentials among the sub-electrodes within a driving unit, the contact angle change occurs only at the bottom right solid-liquid interface (as shown in figure 4(*b*)), unlike a typical top–bottom electrode configuration of figure 1(*b*), where the top two end interfaces and right bottom interface have contact angle changes. The driving pressure in the droplet on the co-planar electrodes under the parallel-plate configuration can finally be related to the contact angle changes through the Laplace equation as

$$\Delta P = \frac{\varepsilon_r \varepsilon_0}{2td}\left(\frac{A_d}{A_t}\left(\frac{A_r}{A_d + A_r}\right)^2 + \frac{A_r}{A_t}\left(\frac{A_d}{A_d + A_r}\right)^2\right)V^2 \quad (4)$$

where ΔP is the internal pressure difference and d is the height of the channel defined by the gap between the two plates.

2.3. *Driving a droplet on coplanar electrodes in an open-plate configuration with no cover plate*

Driving of a sessile droplet on coplanar electrodes in an open-plate configuration (i.e., no cover plate) is schematically illustrated in figure 4(*c*). The maximum driving force is achieved through the same optimizing scheme for the electrode design described above, since the internal pressure gradient is directly proportional to the contact angle changes. However, the droplet changes its shape into complex geometries with varying internal pressure distribution, and a simplified expression for the net driving pressure cannot easily be found, calling for a numerical simulation to obtain a solution.

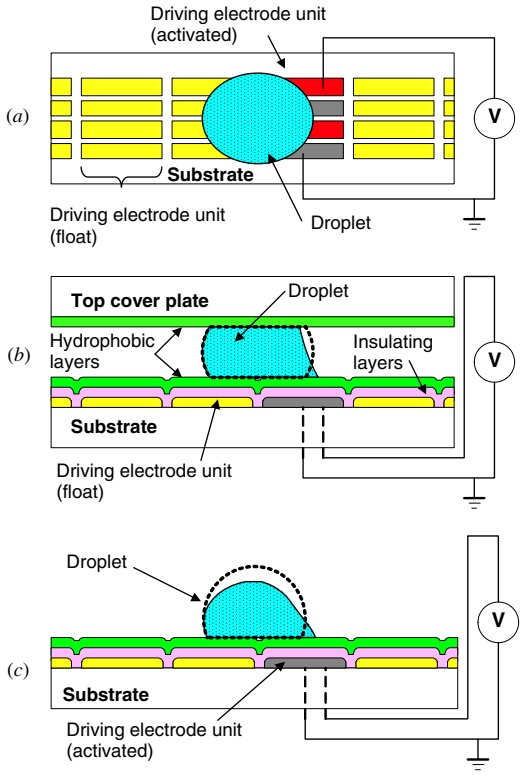

Figure 4. Droplet moving by EWOD on coplanar electrodes. (*a*) Top view showing driving electrode units, each consisting of sub-electrodes (four in this figure). (*b*) Driving in parallel-plate configuration with the top plate having no electrode. (*c*) Driving in open-plate configuration (i.e., no cover plate). Note the initial shapes of droplets before contact angle changes for the two cases, drawn with broken lines.

2.4. Experimental design and fabrications

To demonstrate and characterize EWOD on single-side coplanar electrodes, we designed two main experiments: contact angle measurement and droplet actuation. For the contact angle measurement tests, a sessile drop of deionized (DI) water was placed on a radial pattern of electrodes coated with dielectrics, as shown in figure 3. The radial pattern keeps the contact angles along the edge of a droplet symmetric while voltages are applied. Keeping the areas of the two electrodes equal, the gap areas between them were varied. Chips with 2%, 10%, 20%, 40% and 60% gap areas were designed to find the effect of varying ratios, the 2% gap mimicking the limiting case of no gap within the measurement error. For the droplet actuation tests, three different types of chips were designed, each with a set of two, four or six individually addressable sub-electrodes comprising a driving unit (or pad), as shown in figure 4(*a*) for a set of four. For each design, the gap areas were minimized within our fabrication limitation (typically ∼4 μm line gap) to maximize the EWOD driving force. Each actuation pad is 1.4 mm by 1.4 mm in size, and the sizes of sub-electrodes are adjusted to fit in the pad size.

Both the contact angle measurement chips and the droplet movement chips were designed and fabricated to have identical layers. The chips were micromachined with 4 inch Borofloat® glass wafers. For the metal layer, ∼50 Å chromium and ∼1000 Å gold were evaporated successively and patterned

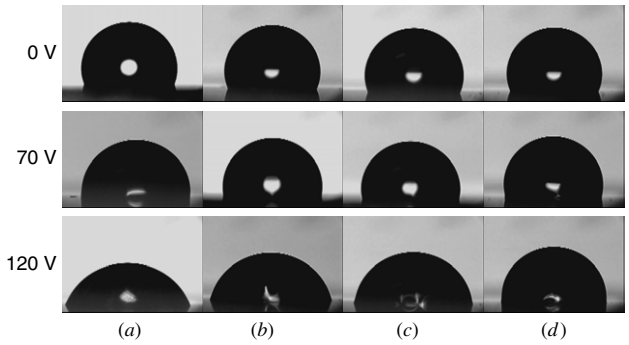

Figure 5. Contact angles of sessile drops on coplanar electrodes of figure 3 for four different gap areas under EWOD actuation. (*a*) 2% gap area, (*b*) 20% gap area, (*c*) 40% gap area, (*d*) 60% gap area.

to define the electrodes and the gaps between the electrodes. For the insulating layer, ∼3000 Å silicon dioxide (SiO_2) was deposited by plasma-enhanced chemical vapor deposition, followed by spin-coating of ∼2000 Å Cytop® to form the top hydrophobic layer. For the passive top plate in figure 4(*b*), no conductive layer was deposited and only Cytop® (∼2000 Å) was spin-coated as a hydrophobic layer.

3. Experiment and result

3.1. Contact angle measurement

The contact angles of a small sessile drop (∼5 μl) of DI water under EWOD actuation by coplanar electrodes were measured optically using a First Ten Angstroms (FTA® 4000A) system. Unlike the tests in Moon *et al* [21], no platinum referencing wire was inserted into the droplet because the reference electrodes are included in the coplanar electrodes on the chip. Only direct current (dc) voltages were used in the tests for accurate measurements, since alternating current (ac) voltages would change the menisci continuously and obstruct clear pictures. The pictures and data obtained from the experiments are shown in figures 5 and 6. Parabolic decreases in contact angles by the increase in applied voltages were observed, as expected from equation (3). The resulting contact angles of each type of the chips are in relatively good agreement with the equation. The highest and lowest changes in the contact angle were observed with 2% and 60% gap areas, respectively, as predicted, and the results quantified the influence of the gap area on the EWOD actuation. For 120 V_{dc} applied, the contact angles of water on 2% chips dropped from ∼108° to ∼68°, while those on 60% chips dropped from ∼108° to only ∼92°. The results show that it is important to minimize the gap area to design effective coplanar EWOD devices.

During the contact angle measurement tests, we have not observed the contact angle saturation phenomenon, previously reported through several papers [21–25]. The resulting contact angles (∼68° for 2% gap) at ∼120 V_{dc} were below the saturation values reported by Moon *et al* (∼75° with ∼1000 Å) [21], which used similar dielectric layers. Several physical mechanisms for the saturation phenomenon, including a zero solid/liquid surface energy limit [22], a charge trapping [23], a material deficiency [24] and ionization of air [25], were proposed. However, the models proposed are mostly inconclusive or specific to the systems studied, and the

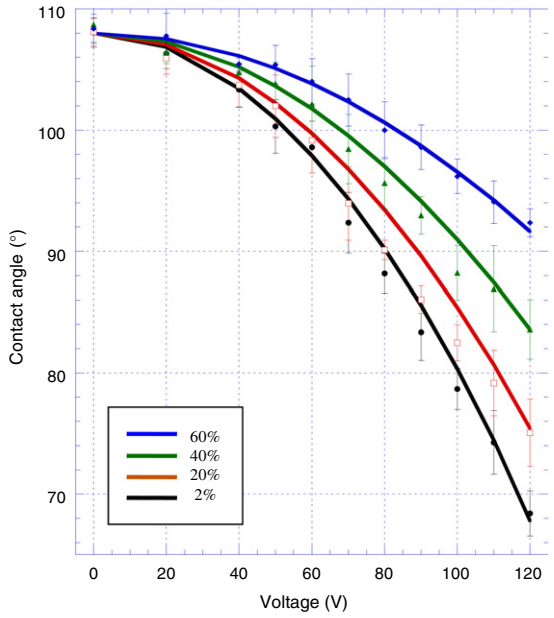

Figure 6. Contact angle changes for EWOD on coplanar electrodes with 2%, 20%, 40% and 60% gap areas. Theoretical values (by equation (3)) are plotted with solid lines while actual data are plotted with geometric dots with error bars ($\pm\sigma$). The data from chips with 10% gap area were also consistent but not plotted in this graph for the readability of data.

phenomenon is yet to be clearly understood. Rather than trying to fit our result to a saturation model, we apply our results to the confirmed dependence on a dielectric layer thickness [21] and suspect the lower contact angles could have been from the thicker dielectric layers (~3000 Å). The applied voltages simply might not have been high enough to cause saturations in our contact angle measurement tests. Higher voltages to reach the possible saturation could not be applied to the chips due to the electrolysis starting around ~125 V. Further investigations including the contact angle measurement with various dielectric thicknesses would be needed to clarify the deviation.

3.2. Moving droplets by EWOD

Coplanar electrode devices with three different numbers (2, 4 and 6) of sub-electrodes were tested for droplet manipulations with a setup consisting of (1) an intermediate testing stage, which provides the electric connections for programmed electrical signals from a custom-made EWOD control circuit board [26] and (2) an optical microscope for visualization. Only ac signals were used for the droplet movement tests to reduce electrolysis on the chip surfaces and for more reliable actuations under varying experiment conditions. Although only ac signals were used, the equations derived previously are still valid for estimating the transportation by EWOD. Using V_{rms}, contact angle changes can be estimated since equivalent values of V_{dc} brings the same energy to the system. It was also observed that about the same V_{rms} are required for EWOD actuations compared to the actuations by V_{dc}. All the values of ac voltages are reported in rms in this paper. The frequency of the signal was fixed at 1 kHz for all the tests for EWOD actuations of droplets with and without cover plates.

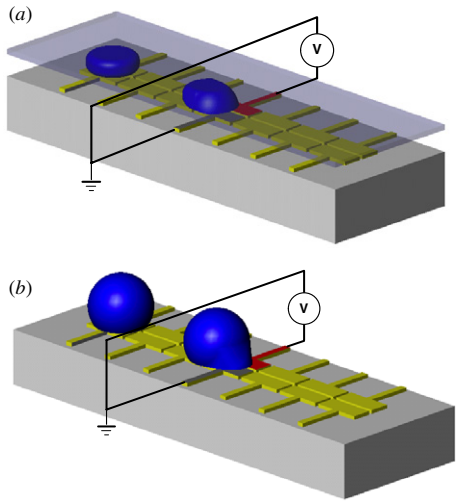

Figure 7. Droplet movement by EWOD on single-side coplanar electrodes, each unit consisting of two sub-electrodes in this figure: (*a*) with top cover plate (i.e., droplet squeezed to a disk shape); and (*b*) with no cover plate (i.e., droplet formed to a spherical shape).

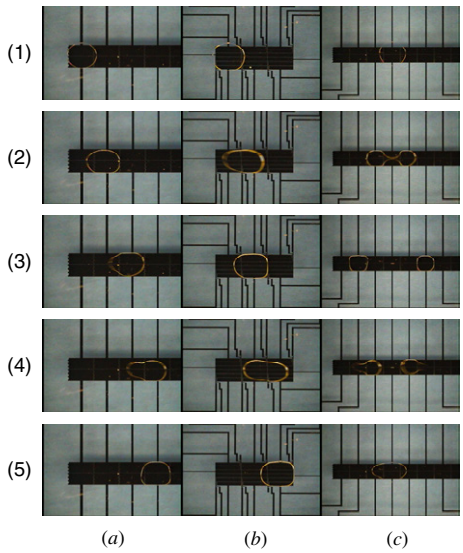

Figure 8. Transportation of a droplet by EWOD on coplanar electrodes under parallel-plate configuration: (*a*) transportation on two-sub-electrode pads; (*b*) transportation on six-sub-electrode pads; (*c*) cutting and merging of a droplet on two-sub-electrode pads.

The tests were done with and without a top cover plate, as schematically illustrated in figure 7. Note that the bottom glass plate, containing both driving and reference electrodes covered with insulating layers, provides all the EWOD actuations. In the parallel-plate configuration of figure 7(*a*), the top glass plate, containing no electrodes and only hydrophobically coated, has only a passive role of squeezing DI water droplets (~0.1 μl) into a disk shape. The channel height (~100 μm) is controlled by spacers between the plates.

Operations were demonstrated as summarized in figure 8. All devices with three different numbers of sub-electrodes (two and six sub-electrodes shown in the figure) were able to move the droplets with minimum applied voltages of ~60 V_{ac}. With ~65 V_{ac}, droplet movements were found

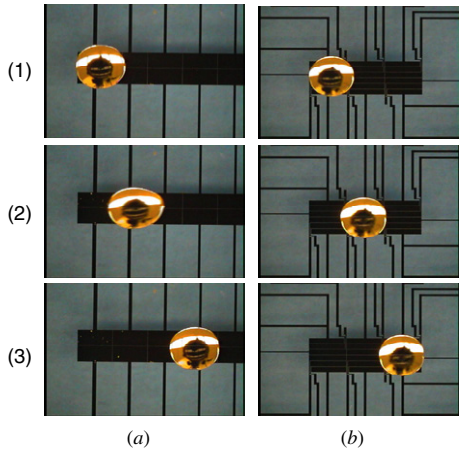

Figure 9. Manipulation of a droplet by EWOD on single-side coplanar electrodes on the open surface (i.e., no cover plate). The droplet volume is ∼2 μl, which is ∼20 times that of figure 8. (*a*) Transportation on two-sub-electrode pads; (*b*) transportation on six-sub-electrode pads.

more reliable over the entire driving pads without a failure. Keeping the ratios of the gap areas to the electrode areas in all three cases of sub-electrodes to minimal (i.e. from ∼0.2% for two-sub-electrode pads to ∼1.4% for six-sub-electrode pads), we found no effect of the number of sub-electrodes per pad on EWOD operations; all three types performed without detectable differences and moving at ∼4.5 mm s^{-1} under given voltages (∼65 V_{ac}). In addition to droplet transportation, splitting and merging of the droplets were also tested (figure 8(*c*)), as described in Cho *et al* [10]. Although the same voltages as transportation tests (∼65 V_{ac}) worked for most cases, the split/merge operations in the figure were obtained by applying higher voltages (75–80 V_{ac}) for reliable repeated operations.

Lastly, devices with interdigitated fingers [8, 9] between two adjacent actuation pads were also tested to see the effect of the fingers on actuations. However, we have not observed any difference between normal electrode patterns (i.e. straight edges) and interdigitated patterns.

Operations on an open-plate configuration (i.e. no cover plate) were confirmed, as shown in figure 9. The spherical droplet (DI water) on an electrode unit in this configuration is ∼2 μl, much larger than that in the parallel-plate configuration (∼0.1 μl). All devices with three different numbers of sub-electrodes (two and six sub-electrodes shown in the figures) were able to move the droplets at ∼10 mm s^{-1} with ∼65 V_{ac}. Droplets move faster in the open-plate configuration because the resistance by the top plate does not exist and the droplets can roll. In the open-plate configuration, a droplet cannot be split in the same fashion. A droplet needs to be squeezed enough between two plates to be cut actively by EWOD actuation [10], which is not possible with one plate. Instead, a passive method may be used on the open surface. A column of liquid should first be formed on the surface, and the column is then cut into multiple droplets by hydrodynamic instability. Typically employed in the dielectrophoretic (DEP) droplet microfluidics [7], this passive cutting method is limited to liquid columns and cannot be applied to droplets. Conversely, a liquid cannot be cut passively by this instability in the parallel-plate configuration even from a columnar shape.

For an open-plate configuration, the evaporation of liquid could be a concern for future device developments. While evaporation is minimized in a closed-plate configuration that exposes only the droplet sides to air [8], it is much faster for a sessile drop in an open-plate configuration. The evaporation can be minimized by operating the droplets in an oil environment [9] or in a humid environment. The humidity can be provided by sealing the plate [16] or placing the device in a chamber with a humidity control. In a sealed device, it was observed that a ∼1.2 μl droplet loses ∼15% of its volume after 8 days.

Without the need for accurate spacing between the top and bottom plates, the droplet volumes are determined only by the electrode sizes, which are defined by photolithography, allowing smaller droplets, if necessary. Be reminded, however, that the volume of sessile droplets varies much more than that of disk-shape droplets in the parallel-plates. We envision that a microfluidic system incorporating both open-plate and parallel-plate configurations can enhance the detection and liquid handling by allowing much greater flexibility in system design and moving various volumes of liquid with the same electrode designs.

4. Conclusions

We have characterized the EWOD actuation on coplanar electrodes through the measurement of contact angle changes and demonstrated the operations with devices. The contact angle changes with corresponding electrode designs were obtained through an optical measurement system and compared with an analytical model. The basic digital fluidic operations (e.g. moving, splitting and merging) have been demonstrated in a parallel-plate configuration, where one plate has no electrodes. The driving of droplets in the open-plate configuration with no cover plate has also been demonstrated. The results verify that the EWOD devices can be made with all the electrodes on one plate, opening the door for lab-on-a-chip systems incorporating various sensing schemes.

Acknowledgments

This work was supported by NASA through the Institute for Cell Mimetic Space Exploration (CMISE) at UCLA. The authors would like to thank Dr Hyejin Moon and Professor Robin L Garrell for their valuable discussions and suggestions for contact angle measurement tests. We also would like to thank Jian Gong for sharing his experimental data about droplet evaporation.

References

[1] Erickson D and Li D 2003 Integrated microfluidic devices *Anal. Chim. Acta* **507** 11–26
[2] Reyes D R, Lossifidis D, Auroux P-A and Manz A 2002 Micro total analysis systems: 1. Introduction, theory and technology *Anal. Chem.* **74** 2623–36
[3] Jun T K and Kim C-J 1998 Valveless pumping using traversing vapor bubbles in microchannels *J. Appl. Phys.* **83** 5658–64

[4] Sammarco T S and Burns M A 1999 Thermalcapillary pumping of discrete drops in microfabricated analysis devices *AIChE J.* **45** 350–66
[5] Strobl C J, Rathgeber A, Wixforth A, Gauer C and Scriba J 2002 Planar microfluidic processors *Proc. IEEE Ultrasonics Symp. (Munich, Germany)* vol 1 pp 255–8
[6] Washizu M 1998 Electrostatic actuation of liquid droplets for microreactor applications *IEEE Trans. Ind. Appl.* **34** 732–7
[7] Jones T B, Gunji M, Washizu M and Feldman M J 2001 Dielectrophoretic liquid actuation and nanodroplet formation *J. Appl. Phys.* **89** 1441–8
[8] Lee J, Moon H, Fowler J, Schoellhammer T and Kim C-J 2002 Electrowetting and electrowetting-on-dielectric for microscale liquid handling *Sensors Actuators* A **95** 259–68
[9] Pollack M G, Shenderov A D and Fair R B 2002 Electrowetting-based actuation of droplets for integrated microfluidics *Lab Chip* **2** 96–101
[10] Cho S K, Moon H and Kim C-J 2003 Creating, transporting, cutting, and merging liquid droplets by electrowetting-based actuation for digital microfluidic circuits *J. Microelectromech. Syst.* **12** 70–80
[11] Fowler J, Moon H and Kim C-J 2002 Enhancement of mixing by droplet-based microfluidics *Proc. Conf. IEEE MEMS (Las Vegas, NV, USA)* pp 97–100
[12] Paik P, Pamula V K and Fair R B 2003 Rapid droplet mixers for digital microfluidic systems *Lap Chip* **3** 253–9
[13] Cho S K and Kim C-J 2003 Particle separation and concentration control for digital microfluidic systems *Proc. Conf. IEEE MEMS (Kyoto, Japan)* pp 686–9
[14] Yi U-C and Kim C-J 2004 Soft printing of droplets pre-metered by electrowetting *Sensors Actuators* A **114** 347–54
[15] Fan S K, de Guzman P-P and Kim C-J 2002 EWOD driving of droplet on NxM grid using single-layer electrode patterns *Tech. Dig. Solid State Sensor, Actuator, and Microsystems Workshop (Hilton Head Island, SC, USA)* pp 134–7
[16] Gong J, Fan S K and Kim C-J 2004 Portable digital microfluidics platform with active but disposable lap-on-chip *Proc.Conf. IEEE MEMS (Maastricht, the Netherlands)* pp 355–8
[17] Kim C-J 2001 Integrated digital microfluidic circuits operated by electrowetting-on-dielectrics (EWOD) principle *BIOFLIPS Program Summary Book: DARPA/MTO Principle Investigators' Meeting (Isle of Palms, SC, USA)* pp 32–3
[18] Yi U-C and Kim C-J 2005 EWOD actuation with electrode-free cover plate *Tech. Dig. Transducers 2005: 13th Int. Conf. on Solid-State Sensors, Actuators and Microsystems (Seoul, Korea)* vol 1 pp 89–92
[19] Berge B 1993 Electrocapillarity and wetting of insulator films by water *C. R. Acad. Sci., Paris* II **317** 157–63
[20] Kwon S and Lee L 2001 Focal length control by microfabricated planar electrodes-based liquid lens (μPELL) *Tech. Dig. Transducers 2001: 11th Int. Conf. on Solid-State Sensors, Actuators and Microsystems (Munich, Germany)* pp 1348–51
[21] Moon H J, Cho S K, Garell R L and Kim C-J 2002 Low voltage electrowetting-on-dielectric *J. Appl. Phys.* **92** 4080–7
[22] Peykov V, Quinn A and Ralston J 2000 Electrowetting: a model for contact-angle saturation *Colloid Polym. Sci.* **278** 789–93
[23] Verhdijen H J J and Prins M W J 1999 Reversible electrowetting and trapping of charge: model and experiments *Langmuir* **15** 6616–20
[24] Seyrat E and Hayes R 2001 Amorphous fluoropolymers as insulators for reversible low-voltage electrowetting *J. Appl. Phys.* **90** 1383–6
[25] Vallet M, Vallade M and Berge B 1999 Limiting phenomena for the spreading of water on polymer films by electrowetting *Eur. Phys. J.* B **11** 583–91
[26] Lee J 2000 Microactuation by continuous electrowetting and electrowetting: theory, fabrication, and demonstration *PhD Dissertation, University of California, Los Angeles, CA, USA*